Frost flowers growing in the Arctic ocean-atmosphere–sea ice–snow interface: 2. Mercury exchange between the atmosphere, snow, and frost flowers

Laura S. Sherman,[1] Joel D. Blum,[1] Thomas A. Douglas,[2] and Alexandra Steffen[3]

Received 2 May 2011; revised 28 September 2011; accepted 30 September 2011; published 9 February 2012.

[1] Frost flowers are ice crystals that grow on refreezing sea ice leads in Polar Regions by wicking brine from the sea ice surface and accumulating vapor phase condensate. These crystals contain high concentrations of mercury (Hg) and are believed to be a source of reactive halogens, but their role in Hg cycling and impact on the fate of Hg deposited during atmospheric mercury depletion events (AMDEs) are not well understood. We collected frost flowers growing on refreezing sea ice near Barrow, Alaska (U.S.A.) during an AMDE in March 2009 and measured Hg concentrations and Hg stable isotope ratios in these samples to determine the origin of Hg associated with the crystals. We observed decreasing Δ^{199}Hg values in the crystals as they grew from new wet frost flowers (mean Δ^{199}Hg = 0.77 ± 0.13‰, 1 s.d.) to older dry frost flowers (mean Δ^{199}Hg = 0.10 ± 0.05‰, 1 s.d.). Over the same time period, mean Hg concentrations in these samples increased from 131 ± 6 ng/L (1 s.d.) to 180 ± 28 ng/L (1 s.d.). Coupled with a previous study of Hg isotopic fractionation during AMDEs, these results suggest that Hg initially deposited to the local snowpack was subsequently reemitted during photochemical reduction reactions and ultimately accumulated on the frost flowers. As a result of this process, frost flowers may lead to enhanced local retention of Hg deposited during AMDEs and may increase Hg loading to the Arctic Ocean.

Citation: Sherman, L. S., J. D. Blum, T. A. Douglas, and A. Steffen (2012), Frost flowers growing in the Arctic ocean-atmosphere–sea ice–snow interface: 2. Mercury exchange between the atmosphere, snow, and frost flowers, *J. Geophys. Res.*, *117*, D00R10, doi:10.1029/2011JD016186.

1. Introduction

[2] During spring in Polar Regions, chemical reactions involving reactive halogens cause atmospheric boundary layer ozone depletion and the oxidation of gaseous elemental mercury (GEM) to reactive gaseous mercury (RGM) and particle-bound mercury (PHg) compounds that are rapidly deposited to the snowpack [*Schroeder et al.*, 1998; *Lu et al.*, 2001; *Ariya et al.*, 2002; *Lindberg et al.*, 2002; *Shepler and Peterson*, 2003; *Steffen et al.*, 2003; *Goodsite et al.*, 2004; *Skov et al.*, 2004; *Brooks et al.*, 2006]. During these atmospheric mercury depletion events (AMDEs), atmospheric boundary layer concentrations of GEM decrease from ~1.6 ng/m^3 to well below 1.0 ng/m^3 for hours to days [*Lindberg et al.*, 2002; *Temme et al.*, 2003; *Skov et al.*, 2004; *Brooks et al.*, 2006]. When these events occur due to local GEM oxidation and deposition rather than influx of a previously depleted air mass [*Gauchard et al.*, 2005], mercury (Hg) concentrations in surface snow can increase by more than an order of magnitude to values as high as 400 ng/L [*Douglas et al.*, 2005; *Johnson et al.*, 2008]. Recent studies including several conducted in Barrow, Alaska (AK) (U.S.A.) [*Brooks et al.*, 2006; *Skov et al.*, 2006; *Johnson et al.*, 2008; *Sherman et al.*, 2010] suggest that a significant portion of the Hg deposited during AMDEs is subsequently reduced during photochemical reactions and reemitted as GEM [*Lalonde et al.*, 2002; *Steffen et al.*, 2002; *Poulain et al.*, 2004; *Kirk et al.*, 2006]. However, the percent of AMDE-deposited Hg remaining in the snowpack at the time of snowmelt has been debated [*Lu et al.*, 2001; *Dommergue et al.*, 2003; *Larose et al.*, 2010; *Sherman et al.*, 2010]. A more complete understanding of Hg cycling at snow and sea ice surfaces during these events is crucial to determining the potential impact of AMDEs on Arctic ecosystems.

[3] The occurrence of locally produced AMDEs requires sunlight, relatively calm meteorological conditions and elevated levels of tropospheric halogens such as bromine (Br) [*Barrie et al.*, 1988; *Fan and Jacob*, 1992; *Lindberg et al.*, 2002]. While the exact mechanisms that cause the production of large quantities of sea salt aerosols during these

[1]Department of Earth and Environmental Sciences, University of Michigan, Ann Arbor, Michigan, USA.
[2]U.S. Army Cold Regions Research and Engineering Laboratory, Fort Wainwright, Alaska, USA.
[3]Air Quality Research Division, Environment Canada, Toronto, Ontario, Canada.

0148-0227/12/2011JD016186

events remain unclear [*Simpson et al.*, 2005], it has been suggested that first-year sea ice [*Simpson et al.*, 2007], blowing snow [*Yang et al.*, 2010], halogen reactivation and emission from snow surfaces [*Piot and von Glasow*, 2008], and frost flowers [*Rankin et al.*, 2002; *Kaleschke et al.*, 2004] are potential sources of the gas-phase halogens. Frost flowers are ice crystals that commonly develop on the surface of new sea ice that is refreezing over leads [*Perovich and Richter-Menge*, 1994; *Martin et al.*, 1996; *Rankin et al.*, 2002; *Douglas et al.*, 2012]. Brine is wicked upward into the newly forming "wet" frost flowers until it is depleted from the ice surface [*Domine et al.*, 2005; *Douglas et al.*, 2012]. The then "dry" frost flowers continue to grow via condensation of water vapor from the supersaturated air directly above the sea ice [*Andreas et al.*, 2002; *Domine et al.*, 2005]. This vapor phase deposition onto the frost flowers generally dilutes the concentrations of major elements (including Cl, Br, Na, K, Mg, and Ca) in the crystals [*Douglas et al.*, 2012]. Frost flowers are eventually buried by blowing snow, flooded with seawater [*Perovich and Richter-Menge*, 1994], or redistributed onto the ice and snowpack by strong winds [*Rankin et al.*, 2002].

[4] In addition to potentially enhancing the production of gas-phase halogens during AMDEs, frost flowers may play other important roles in Arctic Hg cycling. High Hg concentrations have been measured in frost flowers (>150 ng/L) [*Douglas et al.*, 2005, 2008] and it has been suggested that the high halogen concentrations in these ice crystals [*Rankin et al.*, 2002] cause them to scavenge atmospheric Hg [*Douglas et al.*, 2005]. The extent to which frost flowers impact the cycling of Hg between snow, the atmosphere, and sea ice during AMDEs is not well understood. Measurement of Hg stable isotope fractionation has been shown to be an effective tool to study the transfer of Hg between snow and the atmosphere in Arctic regions [*Sherman et al.*, 2010]. As part of the 2009 Ocean-Atmosphere-Sea Ice-Snow (OASIS) field campaign, we measured Hg stable isotope ratios in samples collected near Barrow, AK to investigate the transfer of Hg between frost flowers, surface snow, and the atmospheric boundary layer during polar springtime.

2. Mercury Stable Isotopes

[5] The measurement of Hg stable isotope ratios in natural samples has recently provided insight into Arctic Hg cycling [*Sherman et al.*, 2010; *Point et al.*, 2011]. There are seven stable isotopes of Hg (196, 198, 199, 200, 201, 202, and 204 amu) and isotopic fractionation can occur during a variety of biotic and abiotic reactions. Mercury isotope ratios are reported using delta notation as

$$\delta^{xxx}\mathrm{Hg}\ (‰) = \left(\left[\left(^{xxx}\mathrm{Hg}/^{198}\mathrm{Hg}\right)_{\mathrm{sample}} \Big/ \left(^{xxx}\mathrm{Hg}/^{198}\mathrm{Hg}\right)_{\mathrm{SRM\ 3133}}\right] - 1\right) * 1000 \quad (1)$$

where ^{xxx}Hg is a given isotope of Hg and SRM 3133 is a NIST Hg standard [*Blum and Bergquist*, 2007]. Mass-dependent fractionation (MDF) of Hg can occur during processes such as microbial reduction [*Kritee et al.*, 2007] and photochemical reduction and loss from aqueous solutions and snow [*Bergquist and Blum*, 2007; *Zheng and Hintelmann*, 2009; *Sherman et al.*, 2010]. Mercury can also undergo mass-independent fractionation (MIF), which is reported as the deviation of a measured ratio from that theoretically predicted to result due to kinetic MDF as

$$\Delta^{xxx}\mathrm{Hg} = \delta^{xxx}\mathrm{Hg} - \left(\delta^{202}\mathrm{Hg} * \beta\right) \quad (2)$$

where β is equal to 0.252 for ^{199}Hg and 0.752 for ^{201}Hg [*Blum and Bergquist*, 2007]. MIF can occur during photochemical reactions (due to the "magnetic isotope effect") and to a lesser extent (<~0.5‰) primarily during equilibrium reactions due to differences in the nuclear charge radii between Hg isotopes (the "nuclear field shift effect") [*Bergquist and Blum*, 2007; *Zheng et al.*, 2007; *Estrade et al.*, 2009; *Zheng and Hintelmann*, 2010a]. High levels of MIF occur due to the magnetic isotope effect (MIE) during kinetic photolysis reactions that are spin-selective and involve the creation of long-lived spin-related radical pairs [*Turro*, 1983; *Buchachenko*, 2001; *Bergquist and Blum*, 2007]. Because only the odd-mass-number isotopes of Hg are magnetic and have unpaired nuclear spin, radical pairs involving an odd-mass-number isotope of Hg can recombine at different rates than those with an even-mass-number isotope of Hg. This process has been shown experimentally to produce Δ^{199}Hg/Δ^{201}Hg ratios of between 1.0 and 1.3 [*Bergquist and Blum*, 2007; *Zheng and Hintelmann*, 2009]. During reactions in which radical pairs are generated in the triplet state, triplet to singlet conversion is enhanced by magnetic isotopes. As a result, radical pairs that include odd-mass-number isotopes of Hg recombine at a faster rate and the odd-mass-number isotopes of Hg are preferentially retained as reactants [*Zheng and Hintelmann*, 2010a]. *Bergquist and Blum* [2007] observed this effect during the photochemical reduction of Hg^{2+} from aqueous solutions containing dissolved organic carbon. Because the odd-mass-number isotopes of Hg were preferentially retained in the oxidizing reservoir, positive MIF of ^{199}Hg and ^{201}Hg was observed in the aqueous solutions (Δ^{199}Hg values up to 2.1 ± 0.05‰, 2 s.d.) [*Bergquist and Blum*, 2007]. It is also possible under different bonding conditions for radical pairs that involve Hg to be generated in the singlet state [*Zheng and Hintelmann*, 2010a]. During these reactions, singlet to triplet conversion is enhanced by magnetic isotopes and the recombination of radical pairs that include magnetic isotopes of Hg becomes spin forbidden. This results in the preferential accumulation of the odd-mass-number isotopes of Hg in the reaction products [*Zheng and Hintelmann*, 2010a]. *Sherman et al.* [2010] observed MIF of this character in Arctic snow during an AMDE. Preferential photochemical reduction and loss of the odd-mass-number isotopes of Hg from surface snow resulted in the observation of extreme negative MIF of ^{199}Hg and ^{201}Hg in the snow (Δ^{199}Hg values down to −5.08 ± 0.09‰, 2 s.d.) [*Sherman et al.*, 2010]. This suggests that the measurement of MIF of Hg stable isotopes in Arctic snow and ice samples may help to elucidate the fate of AMDE-deposited Hg.

3. Methods

3.1. Sample Collection

[6] All of the samples described in this study were collected into Teflon bottles (PTFE) using acid-cleaned Teflon scoops. The bottles were acid washed in a clean room in the

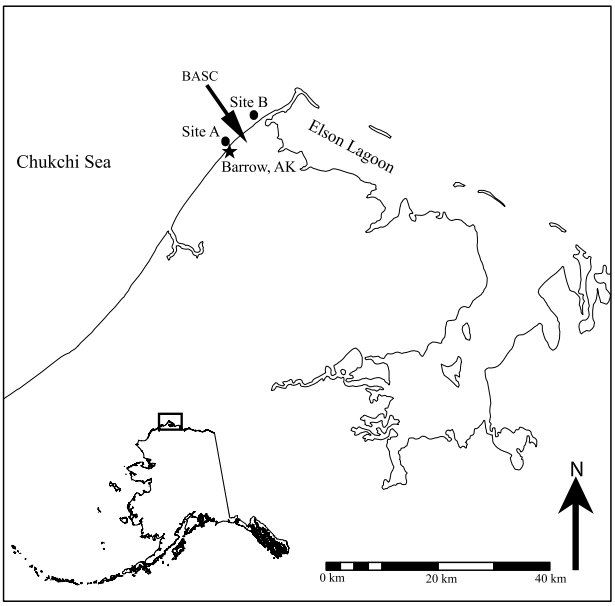

Figure 1. Map of frost flower sampling area near Barrow, AK, with inset map of Alaska. Frost flower sampling locations (Site A: 71.306433 N, 156.807159 W and Site B: 71.35385 N, 156.688171 W) are shown as black dots, the location of Barrow, AK, is shown as a star, and the location of Barrow Arctic Science Consortium (BASC) is indicated with an arrow.

Biogeochemistry and Environmental Isotope Geochemistry Laboratory at the University of Michigan (UM BEIGL). The bottles were fully submerged in a hot 5% HNO_3 (v/v) bath for 48 h and then filled with 5% BrCl (v/v) for 48 h. After being thoroughly rinsed with deionized water, the bottles were dried and a subset were filled with 1% BrCl (v/v), allowed to react for 24 h, and analyzed for Hg concentrations using atomic absorption spectrometry (AAS; Nippon Instruments, MA 2000). Mercury concentrations in these bottle blanks were below the method detection limit (MDL) for these analyses (i.e., <0.76 ng/L; see section 3.2).

[7] As described by *Douglas et al.* [2012], frost flower, snow, and brine samples were collected in March 2009 from two sites located approximately 7 km apart at the edge of the land-fast ice north of Barrow, AK (Figure 1). Site A was located ~3 km northwest of Barrow (71.306433 N, 156.807159 W) and Site B was located ~8.5 km northeast of Barrow (71.35385 N, 156.688171 W). Based on analysis of Moderate Resolution Imaging Spectroradiometer (MODIS) imagery [see *Douglas et al.*, 2012, Figure 1], repeat visits to the sea ice sites, and calm meteorological conditions during the study period, we believe that the frost flowers at the two sites were part of a single large field. This frost flower field was several kilometers long and the ice crystals began growing either in the evening of March 13 or in the morning of March 14 [*Douglas et al.*, 2012]. We collected samples from this field over time to represent a continuum from wet, brine-rich flowers to dry flowers coated with an increasing amount of vapor phase condensate. To ensure collection of sufficient Hg for isotopic analyses, large volume samples were collected at each site when possible. To determine whether AMDEs were occurring during the study period, atmospheric total gaseous Hg (TGM) was measured continuously at the Barrow Arctic Science Consortium (BASC) ~4 km north of Barrow (Figure 1) using a Tekran 2537A. In remote areas such as Barrow where there are no significant local anthropogenic sources of Hg, TGM is predominantly composed of GEM [*Ebinghaus et al.*, 2001; *Douglas et al.*, 2008].

[8] On March 14, 2009, actively growing wet frost flowers were collected at Site A. Based on MODIS imagery, we believe that these frost flowers were less than 24 h old [*Douglas et al.*, 2012]. We also collected frozen surface brine (~3 mm thickness) from an area near these wet frost flowers and older dry frost flowers from a location ~300 m inland. There was no liquid brine at the surface near the dry frost flowers and the crystals were no longer wicking up brine. Finally, we collected surface snow samples (~1 cm in depth) from an ice block elevated 1 m above the sea ice surface near the frost flowers. Although we do not know exactly when this snow began accumulating, clear skies and low winds persisted for several days prior to March 14. Under these cold, clear sky conditions at sites immediately adjacent to open leads and actively refreezing leads, vapor phase deposition of diamond dust and surface hoar can add millimeters to a centimeter of ice crystals to the snowpack surface in a period of less than 24 h [*Douglas et al.*, 2008]. We suggest, therefore, that this snow probably represents a mixture of diamond dust and surface hoar that was less than 24 h old at the time of collection. On March 16, 2009, we returned to Site A and resampled the frost flowers that had been wet and actively taking up brine two days earlier. These frost flowers were dry and had substantially gained in ice volume due to the deposition of vapor phase condensate.

[9] On March 20, 2009, we traveled to Site B and collected dry frost flowers, surface snow and brine samples. As previously discussed, based on MODIS imagery [*Douglas et al.*, 2012], we believe that these frost flowers were part of the same large field as the frost flowers collected at Site A. Therefore, we suggest that these frost flowers were approximately six days old. Finally, in the morning of March 25, 2009 we collected dry frost flowers and brine from a site approximately 1 km south of Site B.

3.2. Analytical Methods

[10] After collection, snow and frost flower samples were kept frozen until they were processed for analysis. At the UM BEIGL, 1% BrCl (v/v) was added to the samples and they were allowed to melt in a clean room. Prior to concentration analysis, 5 ml aliquots of the frost flower and brine samples were treated with ultraviolet light (UV) for three to four days in sealed quartz tubes to release any Hg that was strongly bound to ligands [*Olson et al.*, 1997]. Procedural standards (10 pg of SRM 3133 in 1% BrCl) and blanks were treated with UV light in the same manner. Mercury concentrations were then measured using AAS. Variations in mean concentration measurements are reported as 1 s.d. The MDL for these analyses was 0.76 ng/L (3 s.d. of blank analyses) and all sample replicates were within 11.8% relative percent difference (RPD) (mean RPD = 2.79 ± 2.88%, n = 40). Mercury in procedural standards treated with UV light was consistently recovered after treatment (mean recovery = 100 ± 6%, n = 5) and Hg

Table 1. Hg Concentrations in Frost Flower, Surface Snow, and Brine Samples[a]

Sample Type	Collection Location	Collection Date	[Hg] (ng/L)
Wet frost flowers	Site A	3/14/09	124
Wet frost flowers	Site A	3/14/09	134
Wet frost flowers	Site A	3/14/09	136
Dry frost flowers	Site A	3/14/09	128
Dry frost flowers	Site A	3/14/09	156
Dry frost flowers	Site A	3/14/09	127
Dry frost flowers	Site A	3/14/09	164
Dry frost flowers	Site A	3/14/09	213
Dry frost flowers, 48 h old	Site A	3/16/09	200
Dry frost flowers, 48 h old	Site A	3/16/09	160
Surface snow	Site A	3/14/09	82.3
Surface snow	Site A	3/14/09	92.8
Surface snow	Site A	3/14/09	114
Surface snow	Site A	3/14/09	69.7
Surface snow	Site A	3/14/09	88.0
Brine	Site A	3/14/09	38.5
Brine	Site A	3/14/09	41.4
Brine	Site A	3/14/09	44.5
Dry frost flowers	Site B	3/20/09	51.2
Dry frost flowers	Site B	3/20/09	48.2
Dry frost flowers	Site B	3/20/09	55.4
Dry frost flowers	Site B	3/20/09	42.5
Surface snow	Site B	3/20/09	11.5
Surface snow	Site B	3/20/09	11.3
Brine	Site B	3/20/09	44.8
Brine	Site B	3/20/09	60.7
Frost flowers	1 km S of Site B	3/25/09	91.0
Frost flowers	1 km S of Site B	3/25/09	73.3
Brine	1 km S of Site B	3/25/09	15.9
Brine	1 km S of Site B	3/25/09	16.1

[a]Reported Hg concentrations represent averages of replicate measurements. The MDL for these measurements was 0.76 ng/L and all sample replicates were within 11.8% relative percent difference (RPD) (mean RPD = 2.79 ± 2.88%, n = 40).

concentrations in the procedural blanks treated with UV light were below the MDL (n = 5). Two acid-cleaned bottles were transported to the sampling sites as process bottle blanks and remained closed during the sampling period. These bottles were filled with 200 ml of 1% BrCl (v/v) in a clean room and were found to contain small amounts of Hg (mean = 0.59 ± 0.26 ng per bottle). Although these bottle blanks contain more Hg than the laboratory bottle blanks (which did not contain detectable quantities of Hg), this amount of Hg represents only an average of 2.1 ± 1.1% of the Hg in samples analyzed for isotopic composition and thus is negligible.

[11] After Hg concentration analysis, those samples with sufficient Hg for isotopic analysis (i.e., >8 ng) were concentrated into acidic 1% $KMnO_4$ (w/w) solutions (Alfa Aesar) as follows. Each sample was poured into a 2 L Pyrex bottle and 0.3 mL of 30% NH_2OH HCl (w/v) was added and allowed to react for 30 min. A peristaltic pump was then used to add 100 ml of 5% $SnCl_2$ (w/v) to the solution at a rate of 10 ml/min. Mercury-free air was pulled through the sample and carried the resulting GEM into the trapping solution at a rate of 0.7 L/min for four hours. Procedural standards (25 to 50 ng of SRM 3133 in 1% BrCl) and blanks were processed in the same manner. Mercury in these standards was consistently recovered in the final solutions (mean recovery = 91 ± 6%). The small amount of Hg measured in the procedural blanks (mean = 0.22 ± 0.12 ng per blank, n = 3) was attributable to the $KMnO_4$ solutions. The Hg isotopic compositions of samples and procedural standards were measured using continuous-flow cold vapor generation multicollector inductively coupled plasma mass spectrometry (MC-ICP-MS) according to previously published methods [*Bergquist and Blum*, 2007; *Blum and Bergquist*, 2007].

4. Results

[12] Hg concentrations measured in frost flower, surface snow, and brine samples are presented in Table 1. Frost flowers at Site A increased in Hg concentration as they grew: new wet frost flowers collected on March 14, 2009 contained an average of 131 ± 6 ng/L of Hg, older dry frost flowers collected the same day contained an average 157 ±

Table 2. Hg Isotopic Compositions of Standards and Samples[a]

Sample Type	Collection Location	Collection Date	[Hg] (ng/L)	n	δ^{202}Hg (‰)	2σ (‰)	δ^{201}Hg (‰)	2σ (‰)	δ^{200}Hg (‰)	2σ (‰)	δ^{199}Hg (‰)	2σ (‰)	Δ^{201}Hg (‰)	2σ (‰)	Δ^{200}Hg (‰)	2σ (‰)	Δ^{199}Hg (‰)	2σ (‰)
UM-Almadén standard				36	−0.58	0.07	−0.48	0.09	−0.28	0.07	−0.17	0.08	−0.04	0.06	0.01	0.05	−0.02	0.07
NIST SRM 3133 (snow process std)				3	0.04	0.03	0.04	0.05	−0.03	0.09	−0.03	0.12	0.01	0.03	−0.05	0.11	−0.04	0.13
Wet frost flowers	Site A	3/14/09	124	1	0.36		0.74		0.11		0.95		0.47		−0.07		0.86	
Wet frost flowers	Site A	3/14/09	134	1	0.47		0.74		0.13		0.79		0.39		−0.10		0.67	
Dry frost flowers	Site A	3/14/09	156	2	0.50	0.01	0.46	0.01	0.21	0.06	0.37	0.05	0.09	0.01	−0.04	0.06	0.24	0.05
Dry frost flowers	Site A	3/14/09	213	2	0.59	0.07	0.32	0.05	0.24	0.01	0.20	0.01	−0.12	0.01	−0.06	0.04	0.05	0.00
Dry frost flowers, 48 h old	Site A	3/16/09	200	1	0.49		0.34		0.17		0.26		−0.02		−0.07		0.13	
Dry frost flowers, 48 h old	Site A	3/16/09	160	1	0.53		0.42		0.10		0.19		0.02		−0.17		0.06	
Surface snow	Site A	3/14/09	69.7	1	0.69		−0.48		0.24		−0.83		−1.00		−0.11		−1.01	
Surface snow	Site A	3/14/09	88.0	1	0.63		−0.40		0.3		−0.81		−0.88		−0.02		−0.97	
Dry frost flowers	Site B	3/20/09	51.2	1	−0.28		−0.61		−0.23		−0.43		−0.40		−0.09		−0.36	
Dry frost flowers	Site B	3/20/09	48.2	1	−0.29		−0.35		−0.30		−0.35		−0.14		−0.16		−0.28	
Brine	Site B	3/20/09	60.7	1	−0.39		−0.53		−0.40		−0.49		−0.23		−0.20		−0.39	
Brine	Site B	3/20/09	44.8	1	−0.19		−0.48		−0.11		−0.46		−0.33		−0.01		−0.41	

[a]Presented isotope ratios for the UM-Almadén secondary standard are averages of analytical session averages from January 2010 through March 2011 ("n" is the total number of analytical sessions). Presented isotope ratios for procedural standards are averages of analytical session averages ("n" is the number of processed standards). Number of analysis for samples are the total number of times the sample was analyzed in a single analytical session. Analytical uncertainties for the UM-Almadén standard and procedural standards are 2 s.d. of analytical session averages. Analytical uncertainties presented for limited samples that were measured more than once in a given analytical session are 2 s.d. of analytical session averages. Maximum sample analytical uncertainty for a given isotope ratio is the largest of the uncertainty (2 s.d.) measured in the UM-Almadén standard or procedural standards.

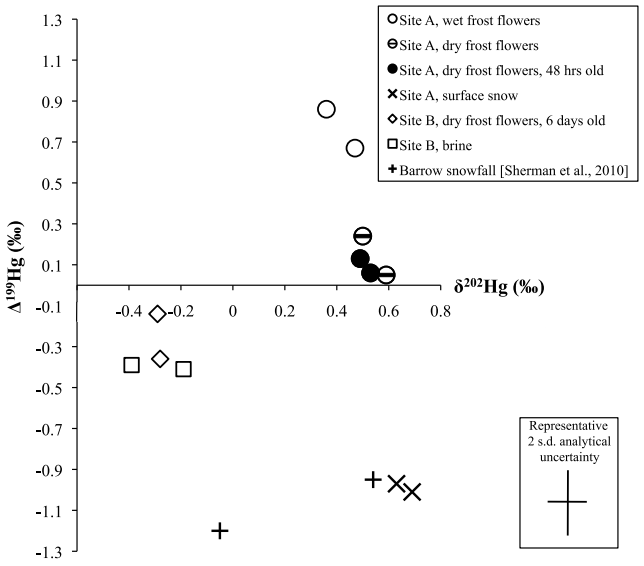

Figure 2. Isotopic composition (δ^{202}Hg versus Δ^{199}Hg) of frost flower, surface snow, and brine samples. Wet frost flowers and surface snow samples were collected at Site A on 3/14/09, dry frost flowers were collected at Site A on 3/14/09 and 3/16/09, and dry frost flowers and brine samples were collected at Site B on 3/20/09. Snowfall samples collected near Barrow, AK, in March 2006 by *Sherman et al.* [2010] are shown as black pluses. Representative sample analytical uncertainty (2 s.d.) is shown.

35 ng/L of Hg, and dry frost flowers that were ~48 h old (collected on March 16) contained an average of 180 ± 28 ng/L of Hg. Surface snow collected on March 14 contained an average of 89.3 ± 16 ng/L of Hg and brine samples scraped from the ice surface on the same day contained lower Hg concentrations (mean = 41.5 ± 3 ng/L). The samples collected from Site B on March 20 contained lower Hg concentrations than the samples collected previously at Site A (dry frost flowers: mean = 49.4 ± 5 ng/L; snow: mean = 11.4 ± 0.2 ng/L; brine: mean = 52.7 ± 11 ng/L). Five days later, Hg concentrations were higher in the dry frost flower samples collected at Site B (mean = 82.2 ± 13 ng/L) but the associated surface brine contained lower Hg concentrations (mean = 16.0 ± 0.1 ng/L).

[13] The isotopic compositions of frost flower, surface snow, and brine samples that contained >8 ng of Hg are presented in Table 2 along with measured isotopic compositions of the UM-Almadén secondary standard and procedural standards. Variations in mean isotope ratios are reported as 1 s.d. As depicted in Figure 2, frost flowers collected at Site A exhibited decreasing Δ^{199}Hg values and slightly increasing δ^{202}Hg values from new wet frost flowers (mean Δ^{199}Hg = 0.77 ± 0.13‰; mean δ^{202}Hg = 0.42 ± 0.08‰) to dry frost flowers that were ~48 h old (mean Δ^{199}Hg = 0.10 ± 0.05‰; mean δ^{202}Hg = 0.51 ± 0.03‰). The dry frost flowers collected on March 14, 2009 (mean Δ^{199}Hg = 0.15 ± 0.13‰; mean δ^{202}Hg = 0.55 ± 0.06‰) were isotopically similar to the dry (~48 h old) frost flowers collected two days later. As discussed previously, the frost flowers at Site A also increased in Hg concentration as they grew (Figure 3). In contrast, surface snow samples collected at Site A displayed negative Δ^{199}Hg values (mean Δ^{199}Hg = −0.99 ± 0.03‰) that were similar to those observed in snowfall samples collected during an AMDE in March 2006 [*Sherman et al.*, 2010] (Figure 2). Frost flowers and brine samples collected at Site B on March 20, 2009 exhibited negative Δ^{199}Hg values (frost flowers: mean Δ^{199}Hg = −0.32 ± 0.06‰; brine: mean Δ^{199}Hg = −0.40 ± 0.01‰) and negative δ^{202}Hg values (frost flowers: mean δ^{202}Hg = −0.29 ± 0.01‰; brine: mean δ^{202}Hg = −0.29 ± 0.14‰).

[14] Interpretation of these data is aided by knowledge of atmospheric TGM concentrations during the study period.

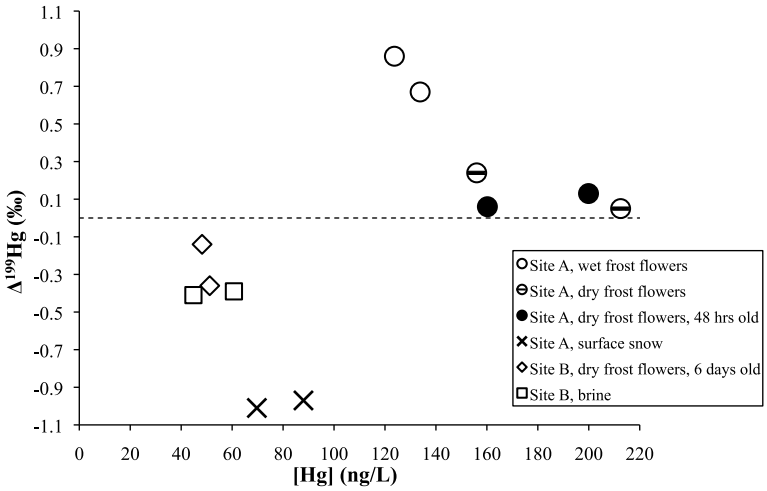

Figure 3. Mercury concentration (ng/L) versus Δ^{199}Hg (‰) for frost flower, surface snow, and brine samples. Wet frost flowers and surface snow samples were collected at Site A on 3/14/09, dry frost flowers were collected at Site A on 3/14/09 and 3/16/09, and dry frost flowers and brine samples were collected at Site B on 3/20/09. Horizontal dashed line depicts the 0 values for the *y* axis.

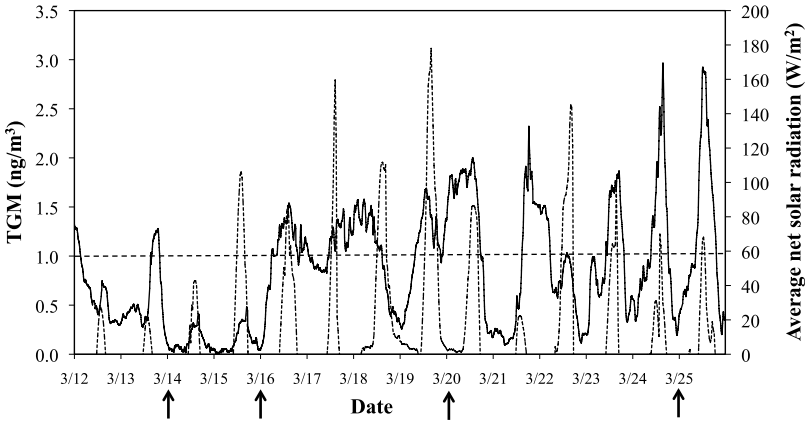

Figure 4. Atmospheric TGM concentrations were measured continuously using a Tekran 2537A at the Barrow Arctic Science Consortium (BASC) located ~4 km north of Barrow, AK. Thirty minute averaged TGM concentrations (ng/m^3, solid black line) and hourly average net solar radiation (W/m^2, dotted black line) from March 12, 2009 through March 25, 2009 are shown. AMDE conditions are characterized by TGM concentrations less than 1.0 ng/m^3 (shown by horizontal dashed line). Sample collection dates are indicated by black arrows (Site A: 3/14/09 and 3/16/09, Site B: 3/20/09 and 3/25/09).

Figure 4 depicts TGM concentrations and average net solar radiation measured at BASC between March 12 and March 25, 2009. Although TGM measurements made at BASC are likely representative of regional atmospheric TGM concentrations, it is possible that TGM concentrations at the sampling sites on the sea ice were somewhat different. However, based on the observed meteorological conditions at BASC, it is likely that the air masses sampled at BASC also impacted the collection sites. From March 14 through March 16 surface winds at BASC were from the east-northeast toward Site A and on March 20 and during the morning of March 25 surface winds at BASC were from the south toward Site B. AMDE conditions existed at BASC while the frost flowers were growing from March 14 to March 16, 2009. During this time period, atmospheric TGM concentrations were highest concurrent with peak solar radiation (Figure 4). This may have occurred due to photochemical reduction and reemission of GEM from the surface snow during the AMDE [*Brooks et al.*, 2006; *Johnson et al.*, 2008]. Atmospheric TGM concentrations began to return to typical background levels (~1.6 ng/m^3) on March 16, 2009 and largely remained at those concentrations until March 19, 2009 when they dropped below 1 ng/m^3 for less than one day. TGM concentrations returned to background concentrations on March 20, 2009 and then oscillated daily between background concentrations and concentrations less than 1 ng/m^3 for the duration of the study period.

5. Discussion

[15] As frost flowers grow, deposition of water vapor condensate causes dilution of major anions and cations in the ice crystals [*Douglas et al.*, 2012]. Our observations of Hg concentrations in frost flowers do not follow this trend. In contrast, as major element concentrations decreased in the frost flowers growing at Site A from March 14 through March 16, 2009 [*Douglas et al.*, 2012], Hg concentrations increased (Figure 3). Previous studies have similarly observed increasing Hg concentrations in frost flowers over time from new wet frost flowers to older dry frost flowers [*Douglas et al.*, 2005, 2008]. Because Hg concentrations are reported as ng of Hg per liter of melted sample, increases in Hg concentration can be the result either of addition of Hg or loss of ice. However, because vapor phase condensate was added to frost flowers collected at Site A as they grew [*Douglas et al.*, 2012], the observed increases in Hg concentration must have been due to the addition of Hg to the frost flowers.

[16] New wet frost flowers collected at Site A on March 14, 2009 displayed positive Δ^{199}Hg values (mean Δ^{199}Hg = 0.77 $\pm$ 0.13‰). It is unlikely that adsorption of RGM to the frost flowers caused MIF via the MIE because photochemical reactions and long-lived radical pairs are not believed to be involved in this process [*Douglas et al.*, 2008]. Although the nuclear field shift (NFS) effect has been observed to cause MIF of Hg during equilibrium reactions, this effect has not been predicted or observed to produce MIF greater than ~0.5‰ [*Schauble*, 2007; *Bergquist and Blum*, 2009; *Estrade et al.*, 2009; *Zheng and Hintelmann*, 2010b]. In addition, the NFS effect has been theoretically predicted and experimentally demonstrated to produce a Δ^{199}Hg/Δ^{201}Hg ratio between 1.6 and 2.5 [*Schauble*, 2007; *Estrade et al.*, 2009; *Zheng and Hintelmann*, 2009, 2010b]. Based on a York regression [*York*, 1966], the frost flower and surface snow samples collected at Site A were characterized by a Δ^{199}Hg/Δ^{201}Hg ratio of 1.26 $\pm$ 0.10 (1 s.d.). Therefore, it is unlikely that adsorption of RGM to the frost flowers caused MIF either via the MIE or the NFS effect. Instead, it is likely that the Hg in the wet frost flowers at Site A exhibited positive MIF prior to adsorption.

[17] There are at least two processes that could produce the Hg that was adsorbed to the frost flowers as they grew: (1) oxidation of background atmospheric GEM or (2) oxidation of GEM emitted from the snowpack surface during photochemical reduction reactions. The oxidation of atmospheric GEM to RGM and subsequent complete deposition of Hg from the atmospheric boundary layer should not cause

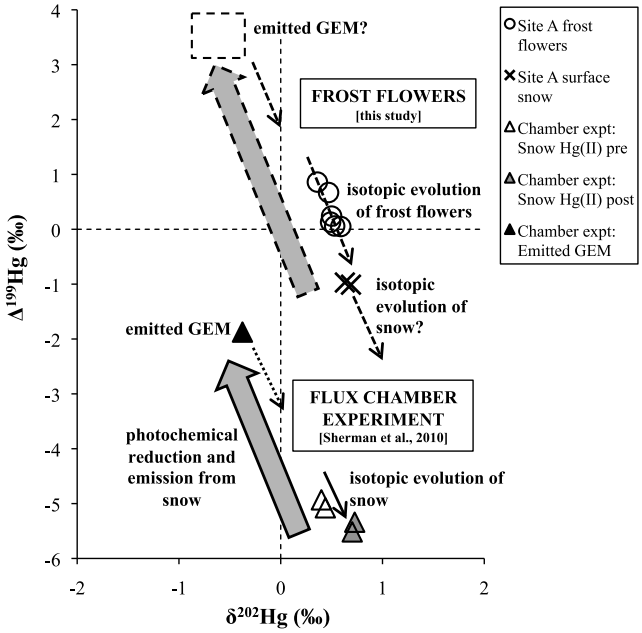

Figure 5. Hypothesized isotopic evolution of frost flower samples, surface snow, and emitted GEM. Symbols for frost flower and surface snow samples collected at Site A during this study are shown in the figure legend. Samples collected during a flux chamber experiment conducted by *Sherman et al.* [2010] are shown as triangles where drifted snow originally placed in the chamber are open triangles, snow after the experiment are gray triangles, and emitted GEM is a black triangle. Fractionation observed during that experiment is shown as a large solid gray arrow. Hypothesized fractionation occurring during photochemical reduction and emission of Hg from snow during this study is shown as a large dashed gray arrow and the hypothesized isotopic composition of GEM initially emitted by the surface snow is shown as a dashed box. Horizontal dashed lines depict the 0 values for both axes.

MIF of Hg isotopes. During the AMDE that began on March 14, 2009, atmospheric GEM concentrations dropped to less than 0.1 ng/m^3 (Figure 4). Due to mass balance, such complete Hg deposition should result in preservation of the isotopic composition of atmospheric GEM in the deposited Hg [*Sherman et al.*, 2010]. Background TGM collected in Barrow, AK in June 2008 did not display positive Δ^{199}Hg values (Δ^{199}Hg = −0.11 and −0.22 ± 0.08‰, 2 s.d. [*Sherman et al.*, 2010]). Based on this evidence, we argue that complete depletion of atmospheric Hg during AMDEs results in deposition of Hg that does not display positive MIF.

[18] However, if atmospheric depletion of Hg is not complete and oxidation of GEM to RGM during AMDEs causes positive MIF, background atmospheric Hg deposited during AMDEs might display positive MIF. Several studies have investigated the reactions that result in the oxidation of GEM to RGM during AMDEs [*Ariya et al.*, 2002; *Lindberg et al.*, 2002; *Calvert and Lindberg*, 2003; *Goodsite et al.*, 2004; *Skov et al.*, 2006]. Although this oxidation may occur through several reaction pathways, kinetic and thermodynamic studies, ab initio calculations, and measured atmospheric halogen concentrations during AMDEs indicate that gaseous atomic Br is one of the most significant oxidizing agents [*Ariya et al.*, 2002; *Lindberg et al.*, 2002; *Khalizov et al.*, 2003; *Shepler and Peterson*, 2003; *Goodsite et al.*, 2004; *Xie et al.*, 2008]. GEM oxidation by gaseous Br may proceed according to reactions such as the following:

$$Hg^0 + Br \rightarrow HgBr \quad (3)$$

$$HgBr + Br \rightarrow HgBr_2 \quad (4)$$

[19] Although sunlight is necessary to photolytically produce atomic Br from Br_2, the gas-phase oxidation of Hg^0 by Br (reaction 3) is not a directly photochemically mediated radical pair reaction [*Fan and Jacob*, 1992; *Barrie and Platt*, 1997; *Foster et al.*, 2001; *Goodsite et al.*, 2004; *Brooks et al.*, 2006]. It is possible, however, that the radical pair intermediates in reaction 4 may be relatively long-lived. Therefore, we cannot discount the possibility that reaction 4 may cause MIF via the MIE. However, as discussed previously, because GEM is nearly completely depleted from the atmosphere during AMDEs, it is not likely that deposited RGM retains a significant MIF signature.

[20] Based on these arguments, it is unlikely that RGM produced via oxidation of background atmospheric GEM during the AMDE on March 14, 2009 displayed positive MIF. However, as described above, Hg in wet frost flowers growing at Site A displayed significant positive Δ^{199}Hg values. We infer that RGM deposited to local surface snows was photochemically reduced and reemitted, subsequently locally reoxidized (either by gaseous halogens or heterogeneously on the frost flowers), and adsorbed to the growing frost flowers [*Skov et al.*, 2006]. *Sherman et al.* [2010] observed extreme negative Δ^{199}Hg values in snow samples collected during an AMDE in March 2006. To determine the cause of this fractionation, the authors filled a flux chamber with drifted snow that displayed negative Δ^{199}Hg values (Figure 5). By exposing the snow to sunlight and collecting the emitted GEM, the authors determined that photochemical reduction of Hg in the snow caused the preferential emission of the odd-mass-number isotopes of Hg as GEM [*Sherman et al.*, 2010]. Relative to the Hg originally in the snow, this resulted in more negative Δ^{199}Hg values in the snow after photochemical reduction and less negative Δ^{199}Hg values in the emitted GEM (Figure 5) [*Sherman et al.*, 2010]. Although the authors were able to measure the preferential emission of the odd-mass-number isotopes of Hg during this experiment, they did not observe the retention of this Hg in local snow or any other reservoir [*Sherman et al.*, 2010].

[21] We suggest that frost flowers may adsorb a portion of the Hg that is reemitted from surface snow and locally reoxidized. These crystals thereby represent a complementary isotopic reservoir to surface snow. As shown in Figure 5, if this process occurred in a manner similar to that observed by *Sherman et al.* [2010], we would expect the Δ^{199}Hg value of GEM emitted from the collected surface snow samples was positive (expected Δ^{199}Hg ≈ 3.4‰ based on $\Delta^{199}\alpha_{\text{snow-air}}$ = 0.99660 [*Sherman et al.*, 2010]). As photochemical reduction continued, we expect that Δ^{199}Hg values in the surface snow and emitted GEM decreased

(Figure 5). The reoxidation and adsorption of this Hg to the frost flowers through time would have caused Δ^{199}Hg values in the ice crystals to decrease as Hg was added to them (Figure 5).

[22] It is difficult to estimate when the frost flowers began accumulating Hg and how the rate of Hg adsorption changed through time. Based on the Δ^{199}Hg values measured in frost flowers collected at Site A on March 14, 2009, it is likely that the frost flowers began accumulating Hg after the local surface snow had already lost some Hg. The deposition velocity of RGM depends on a number of factors that may have changed throughout the study period including the meteorology (e.g., wind speed and temperature) and surface properties of the RGM species [*Skov et al.*, 2006]. In addition, as the frost flowers grew and their chemical composition and physical properties changed [*Domine et al.*, 2005; *Douglas et al.*, 2012], their ability to scavenge Hg may have also changed. Because this system is very complex, it is not currently possible to quantitatively model the isotopic evolution of the frost flowers and corresponding surface snow without making an unreasonable number of simplifying assumptions.

[23] In contrast to the frost flowers collected at Site A, frost flowers collected at Site B on March 20, 2009 were characterized by negative δ^{202}Hg values (mean = -0.29 ± 0.01‰), negative Δ^{199}Hg values (Δ^{199}Hg = -0.36 and -0.28 ± 0.18‰, 2 s.d.) and lower Hg concentrations (mean = 49.7 ± 2.1 ng/L). The difference in frost flower δ^{202}Hg values between Sites A and B probably reflects spatial variations in Hg isotopic composition among snow samples which has been observed previously but is not well understood [*Sherman et al.*, 2010]. We suggest that there are several possible explanations for the observed negative Δ^{199}Hg values in the frost flowers at Site B including (1) adsorption of isotopically distinct Hg relative to that adsorbed to frost flowers at Site A, (2) photochemical reduction of Hg from the frost flowers, or (3) continued accumulation of Hg emitted from the snowpack surface coupled with deposition of vapor phase condensate. We cannot rule out the possibility that Hg initially deposited to the frost flowers collected at Site B was different isotopically than Hg initially deposited to frost flowers growing at Site A. However, this seems unlikely because the crystals growing at both sites were part of one large frost flower field [*Douglas et al.*, 2012]. It is possible that photochemical reduction and loss of Hg from the frost flowers could have occurred at Site B after AMDE conditions ended on March 16, 2009. If the Hg bonding environment in these ice crystals is similar to that of Hg in surface snow, we expect that photochemical reduction of Hg from the frost flowers would cause the preferential loss of the odd-mass-number isotopes of Hg and could have resulted in the observed negative Δ^{199}Hg values. However, because frost flowers contain high concentrations of Br [*Perovich and Richter-Menge*, 1994; *Rankin et al.*, 2002; *Douglas et al.*, 2012], it is possible that Hg that is reduced and emitted from the ice crystals may be rapidly reoxidized and readsorbed [*Poulain et al.*, 2004; *Skov et al.*, 2006]. We think it is most likely that frost flowers at Site B continued to accumulate Hg emitted from the local surface snowpack after the dry frost flowers were collected at Site A on March 16. Continued adsorption of this Hg by the frost flowers at Site B could have resulted in the observed negative Δ^{199}Hg values in these samples. After the AMDE ended and atmospheric GEM concentrations returned to background values, water vapor containing little to no Hg may have condensed on the frost flowers at Site B. This would have resulted in decreased Hg concentrations but would not have modified the Hg isotopic composition of the frost flowers.

6. Conclusions

[24] The fate of Hg deposited during AMDEs in Polar Regions is a question of scientific interest. Based on analysis of Hg stable isotopes in frost flowers collected during an AMDE in March 2009, we suggest that Hg accumulating on the crystals was originally deposited to local surface snow. A portion of this Hg was reduced during photochemical reactions, reemitted as GEM, and subsequently locally reoxidized and adsorbed onto the frost flowers. This process likely occurs repeatedly throughout Polar Regions on refreezing sea ice leads during the spring AMDE season. A thinner, more dynamic Arctic sea ice cover is expected in the future [*Haas et al.*, 2008; *Rothrock et al.*, 2008]. This sea ice will likely have more open leads and may yield more new ice and frost flowers. The results of this study suggest that frost flowers may, at least temporarily, aid in the local retention of AMDE-deposited Hg. Ultimately, an increase in conditions that favor frost flower growth in the Arctic may cause an increase in Hg flux to sea ice and to the Arctic Ocean.

[25] **Acknowledgments.** Funding for L. S. Sherman was provided by a National Defense Science and Engineering Graduate Fellowship (DOD-ONR) and the University of Michigan Graham Environmental Sustainability Institute. Funding for J. D. Blum and laboratory support was provided by the John D. MacArthur Professorship at the University of Michigan. Funding for sample collection and research conducted by T. A. Douglas was supported by the U.S. National Science Foundation and the National Aeronautic and Space Administration. Field logistics in Barrow, AK, were provided by the Barrow Arctic Science Consortium and were partially funded by Environment Canada and the Canadian IPY program. We thank two anonymous reviewers for comments that greatly improved this manuscript.

References

Andreas, E. L., P. S. Guest, P. O. G. Persson, C. W. Fairall, T. W. Horst, R. E. Moritz, and S. R. Semmer (2002), Near-surface water vapor over polar sea ice is always near ice saturation, *J. Geophys. Res.*, *107*(C10), 8033, doi:10.1029/2000JC000411.

Ariya, P. A., A. Khalizov, and A. Gidas (2002), Reactions of gaseous mercury with atomic and molecular halogens: Kinetics, product studies, and atmospheric implications, *J. Phys. Chem. A*, *106*, 7310–7320, doi:10.1021/jp020719o.

Barrie, L., and U. Platt (1997), Arctic tropospheric chemistry: An overview, *Tellus, Ser. B*, *49*, 450–454.

Barrie, L. A., J. W. Bottenheim, R. C. Schnell, P. J. Crutzen, and R. A. Rasmussen (1988), Ozone destruction and photochemical reactions at polar sunrise in the lower Arctic atmosphere, *Nature*, *334*, 138–141, doi:10.1038/334138a0.

Bergquist, B. A., and J. D. Blum (2007), Mass-dependent and mass-independent fractionation of Hg isotopes by photo-reduction in aquatic systems, *Science*, *318*(5849), 417–420, doi:10.1126/science.1148050.

Bergquist, B. A., and J. D. Blum (2009), The odds and evens of mercury isotopes: Applications of mass-dependent and mass-independent isotope fractionation, *Elements*, *5*, 353–357, doi:10.2113/gselements.5.6.353.

Blum, J. D., and B. A. Bergquist (2007), Reporting the variations in the natural isotopic composition of mercury, *Anal. Bioanal. Chem.*, *388*(2), 353–359, doi:10.1007/s00216-007-1236-9.

Brooks, S. B., A. Saiz-Lopez, H. Skov, S. E. Lindberg, J. M. C. Plane, and M. E. Goodsite (2006), The mass balance of mercury in the springtime arctic environment, *Geophys. Res. Lett.*, *33*, L13812, doi:10.1029/2005GL025525.

Buchachenko, A. L. (2001), Magnetic isotope effect: Nuclear spin control of chemical reactions, *J. Phys. Chem.*, *105*(44), 9995–10,011, doi:10.1021/jp011261d.

Calvert, J. G., and S. E. Lindberg (2003), A modeling study of the mechanism of the halogen-ozone-mercury homogeneous reactions in the troposphere during the polar spring, *Atmos. Environ.*, *37*, 4467–4481, doi:10.1016/j.atmosenv.2003.07.001.

Domine, F., A. S. Taillandier, W. R. Simpson, and K. Severin (2005), Specific surface area, density and microstructure of frost flowers, *Geophys. Res. Lett.*, *32*, L13502, doi:10.1029/2005GL023245.

Dommergue, A., C. P. Ferrari, P.-A. Gauchard, and C. F. Boutron (2003), The fate of mercury species in a sub-arctic snowpack during snowmelt, *Geophys. Res. Lett.*, *30*(12), 1621, doi:10.1029/2003GL017308.

Douglas, T. A., M. Sturm, W. R. Simpson, S. Brooks, S. E. Lindberg, and D. K. Perovich (2005), Elevated mercury measured in snow and frost flowers near Arctic sea ice leads, *Geophys. Res. Lett.*, *32*, L04502, doi:10.1029/2004GL022132.

Douglas, T. A., M. Sturm, W. R. Simpson, J. D. Blum, L. Alvarez-Aviles, G. J. Keeler, D. K. Perovich, A. Biswas, and K. Johnson (2008), Influence of snow and ice crystal formation and accumulation on mercury deposition to the Arctic, *Environ. Sci. Technol.*, *42*, 1542–1551, doi:10.1021/es070502d.

Douglas, T. A., et al. (2012), Frost flowers growing in the Arctic ocean-atmosphere–sea ice–snow interface: 1. Chemical composition and formation history, *J. Geophys. Res.*, *117*, D00R09, doi:10.1029/2011JD016460.

Ebinghaus, R., H. H. Kock, and S. R. Schmolke (2001), Measurements of atmospheric mercury with high time resolution: Recent applications in environmental research and monitoring, *Fresenius J. Anal. Chem.*, *371*, 806–815, doi:10.1007/s002160101048.

Estrade, N., J. Carignan, J. E. Sonke, and O. F. X. Donard (2009), Mercury isotope fractionation during liquid-vapor evaporation experiments, *Geochim. Cosmochim. Acta*, *73*, 2693–2711, doi:10.1016/j.gca.2009.01.024.

Fan, S.-M., and D. J. Jacob (1992), Surface ozone depletion in Arctic spring sustained by bromine reactions on aerosols, *Nature*, *359*, 522–524, doi:10.1038/359522a0.

Foster, K. L., R. A. Plastridge, J. W. Bottenheim, P. B. Shepson, B. J. Finlayson-Pitts, and C. W. Spicer (2001), The role of Br_2 and BrCl in surface ozone destruction at polar sunrise, *Science*, *291*(5503), 471–474, doi:10.1126/science.291.5503.471.

Gauchard, P.-A., et al. (2005), Study of the origin of atmospheric mercury depletion events recorded in Ny-lesund, Svalbard, spring 2003, *Atmos. Environ.*, *39*(39), 7620–7632, doi:10.1016/j.atmosenv.2005.08.010.

Goodsite, M. E., J. M. C. Plane, and H. Skov (2004), A theoretical study of the oxidation of Hg^0 to $HgBr_2$ in the troposphere, *Environ. Sci. Technol.*, *38*, 1772–1776, doi:10.1021/es034680s.

Haas, C., A. Pfaffling, S. Hendricks, L. Rabenstein, J.-L. Etienne, and I. Rigor (2008), Reduced ice thickness in Arctic Transpolar Drift favors rapid ice retreat, *Geophys. Res. Lett.*, *35*, L17501, doi:10.1029/2008GL034457.

Johnson, K. P., J. D. Blum, G. J. Keeler, and T. A. Douglas (2008), Investigation of the deposition and emission of mercury in arctic snow during an atmospheric mercury depletion event, *J. Geophys. Res.*, *113*, D17304, doi:10.1029/2008JD009893.

Kaleschke, L., et al. (2004), Frost flower on sea ice as a source of sea salt and their influence on tropospheric halogen chemistry, *Geophys. Res. Lett.*, *31*, L16114, doi:10.1029/2004GL020655.

Khalizov, A. F., B. Viswanathan, P. Larregaray, and P. A. Ariya (2003), A theoretical study on the reactions of Hg with halogens: Atmospheric implications, *J. Phys. Chem. A*, *107*(33), 6360–6365, doi:10.1021/jp0350722.

Kirk, J. L., V. L. St. Louis, and M. J. Sharp (2006), Rapid reduction and reemission of mercury deposited into snowpacks during atmospheric mercury depletion events at Churchill, Manitoba, Canada, *Environ. Sci. Technol.*, *40*, 7590–7596, doi:10.1021/es061299+.

Kritee, K., J. D. Blum, M. W. Johnson, B. A. Bergquist, and T. Barkay (2007), Mercury stable isotope fractionation during reduction of Hg(II) to Hg(0) by mercury resistant microorganisms, *Environ. Sci. Technol.*, *41*, 1889–1895, doi:10.1021/es062019t.

Lalonde, J., A. J. Poulain, and M. Amyot (2002), The role of mercury redox reactions in snow on snow-to-air mercury transfer, *Environ. Sci. Technol.*, *36*, 174–178, doi:10.1021/es010786g.

Larose, C., A. Dommergue, M. De Angelis, D. Cossa, B. Averty, N. Marusczak, N. Soumis, D. Schneider, and C. Ferrari (2010), Springtime changes in snow chemistry lead to new insights into mercury methylation in the Arctic, *Geochim. Cosmochim. Acta*, *74*, 6263–6275, doi:10.1016/j.gca.2010.08.043.

Lindberg, S. E., S. Brooks, C.-J. Lin, K. J. Scott, M. S. Landis, R. K. Stevens, M. Goodsite, and A. Richter (2002), Dynamic oxidation of gaseous mercury in the troposphere at polar sunrise, *Environ. Sci. Technol.*, *36*, 1245–1256, doi:10.1021/es0111941.

Lu, J. Y., W. H. Schroeder, L. A. Barrie, and A. Steffen (2001), Magnification of atmospheric mercury deposition to polar regions in springtime: The link to tropospheric ozone depletion chemistry, *Geophys. Res. Lett.*, *28*(17), 3219–3222, doi:10.1029/2000GL012603.

Martin, S., Y. Yu, and R. Drucker (1996), The temperature dependence of frost flower growth on laboratory sea ice and the effect of the flowers on infrared observations of the surface, *J. Geophys. Res.*, *101*(C5), 12,111–12,125, doi:10.1029/96JC00208.

Olson, M. L., L. B. Cleckner, J. P. Hurley, D. P. Krabbenhoft, and T. W. Heelan (1997), Resolution of matrix effects on analysis of total and methyl mercury in aqueous samples from the Florida Everglades, *Fresenius J. Anal. Chem.*, *358*(3), 392–398, doi:10.1007/s002160050435.

Perovich, D., and J. A. Richter-Menge (1994), Surface characteristics of lead ice, *J. Geophys. Res.*, *99*(C8), 16,341–16,350, doi:10.1029/94JC01194.

Piot, M., and R. von Glasow (2008), The potential importance of frost flowers, recycling on snow, and open leads for ozone depletion events, *Atmos. Chem. Phys.*, *8*(9), 2437–2467, doi:10.5194/acp-8-2437-2008.

Point, D., J. E. Sonke, R. D. Day, D. G. Roseneau, K. A. Hobson, S. S. Vander Pol, A. J. Moors, R. S. Pugh, O. F. X. Donard, and P. R. Becker (2011), Methylmercury photodegradation influenced by sea-ice cover in Arctic marine ecosystems, *Nat. Geosci.*, *4*, 188–194, doi:10.1038/ngeo1049.

Poulain, A. J., J. D. Lalonde, M. Amyot, J. A. Shead, F. Raofie, and P. A. Ariya (2004), Redox transformations of mercury in an Arctic snowpack at springtime, *Atmos. Environ.*, *38*, 6763–6774, doi:10.1016/j.atmosenv.2004.09.013.

Rankin, A. M., E. W. Wolff, and S. Martin (2002), Frost flowers: Implications for tropospheric chemistry and ice core interpretation, *J. Geophys. Res.*, *107*(D23), 4683, doi:10.1029/2002JD002492.

Rothrock, D. A., D. B. Percival, and M. Wensnahan (2008), The decline in arctic sea-ice thickness: Separating the spatial, annual, and interannual variability in a quarter century of submarine data, *J. Geophys. Res.*, *113*, C05003, doi:10.1029/2007JC004252.

Schauble, E. A. (2007), Role of nuclear volume in driving equilibrium stable isotope fractionation of mercury, thallium, and other very heavy elements, *Geochim. Cosmochim. Acta*, *71*, 2170–2189, doi:10.1016/j.gca.2007.02.004.

Schroeder, W. H., K. G. Anlauf, L. A. Barrie, J. Y. Lu, A. Steffen, D. R. Schneeberger, and T. Berg (1998), Arctic springtime depletion of mercury, *Nature*, *394*, 331–332, doi:10.1038/28530.

Shepler, B. C., and K. A. Peterson (2003), Mercury monoxide: A systematic investigation of its ground electronic state, *J. Phys. Chem. A*, *107*(11), 1783–1787, doi:10.1021/jp027512f.

Sherman, L. S., J. D. Blum, K. P. Johnson, G. J. Keeler, J. A. Barres, and T. A. Douglas (2010), Mass-independent fractionation of mercury isotopes in Arctic snow driven by sunlight, *Nat. Geosci.*, *3*(3), 173–177, doi:10.1038/ngeo758.

Simpson, W. R., L. Alvarez-Aviles, T. A. Douglas, M. Sturm, and F. Domine (2005), Halogens in the coastal snow pack near Barrow, Alaska: Evidence for active bromine air-snow chemistry during springtime, *Geophys. Res. Lett.*, *32*, L04811, doi:10.1029/2004GL021748.

Simpson, W. R., D. Carlson, G. Honninger, T. A. Douglas, M. Sturm, D. Perovich, and U. Platt (2007), First-year sea-ice contact predicts bromine monoxide (BrO) levels at Barrow, Alaska better than potential frost flower contact, *Atmos. Chem. Phys.*, *7*, 621–627, doi:10.5194/acp-7-621-2007.

Skov, H., J. H. Christensen, M. E. Goodsite, N. Z. Heidam, B. Jensen, P. Wahlin, and G. Geernaert (2004), Fate of elemental mercury in the Arctic during atmospheric mercury depletion episodes and the load of atmospheric mercury to the Arctic, *Environ. Sci. Technol.*, *38*(8), 2373–2382, doi:10.1021/es030080h.

Skov, H., S. B. Brooks, M. E. Goodsite, S. E. Lindberg, T. P. Meyers, M. S. Landis, M. R. B. Larsen, B. Jensen, G. McConville, and J. Christensen (2006), Fluxes of reactive gaseous mercury measured with a newly developed method using relaxed eddy accumulation, *Atmos. Environ.*, *40*(28), 5452–5463, doi:10.1016/j.atmosenv.2006.04.061.

Steffen, A., W. Schroeder, J. Bottenheim, J. Narayan, and J. D. Fuentes (2002), Atmospheric mercury concentrations: Measurements and profiles near snow and ice surfaces in the Canadian Arctic during Alert 2000, *Atmos. Environ.*, *36*, 2653–2661, doi:10.1016/S1352-2310(02)00112-7.

Steffen, A., W. H. Schroeder, G. Edwards, and C. Banic (2003), Mercury throughout polar sunrise 2002, *J. Phys. IV*, *107*, 1267–1270, doi:10.1051/jp4:20030531.

Temme, C., J. W. Einax, R. Ebinghaus, and W. H. Schroeder (2003), Measurements of atmospheric mercury species at a coastal site in the Antarctic and over the South Atlantic Ocean during polar summer, *Environ. Sci. Technol.*, *37*, 22–31, doi:10.1021/es025884w.

Turro, N. J. (1983), Influence of nuclear spin on chemical reactions: Magnetic isotope and magnetic field effects, *Proc. Natl. Acad. Sci. U. S. A.*, *80*, 609–621, doi:10.1073/pnas.80.2.609.

Xie, Z.-Q., R. Sander, U. Poschl, and F. Slemr (2008), Simulation of atmospheric mercury depletion events (AMDEs) during polar springtime using

the MECCA box model, *Atmos. Chem. Phys.*, *8*, 7165–7180, doi:10.5194/acp-8-7165-2008.

Yang, X., J. A. Pyle, R. A. Cox, N. Theys, and M. Van Roozendael (2010), Snow-sourced bromine and its implications for polar tropospheric ozone, *Atmos. Chem. Phys.*, *10*, 7763–7773, doi:10.5194/acp-10-7763-2010.

York, D. (1966), Least-squares fitting of a straight line, *Can. J. Phys.*, *44*, 1079–1086, doi:10.1139/p66-090.

Zheng, W., and H. Hintelmann (2009), Mercury isotope fractionation during photoreduction in natural water is controlled by its Hg/DOC ratio, *Geochim. Cosmochim. Acta*, *73*, 6704–6715, doi:10.1016/j.gca.2009.08.016.

Zheng, W., and H. Hintelmann (2010a), Isotope fractionation of mercury during its photochemical reduction by low-molecular-weight organic compounds, *J. Phys. Chem. A*, *114*(12), 4246–4253, doi:10.1021/jp9111348.

Zheng, W., and H. Hintelmann (2010b), Nuclear field shift effect in isotope fractionation of mercury during abiotic reduction in the absence of light, *J. Phys. Chem. A*, *114*(12), 4238–4245, doi:10.1021/jp910353y.

Zheng, W., D. Foucher, and H. Hintelmann (2007), Mercury isotope fractionation during volatilization of Hg(0) from solution into the gas phase, *J. Anal. At. Spectrom.*, *22*, 1097–1104, doi:10.1039/b705677j.

J. D. Blum and L. S. Sherman, Department of Earth and Environmental Sciences, University of Michigan, 1100 N. University Ave., Ann Arbor, MI 48109, USA. (lsaylors@umich.edu)

T. A. Douglas, U.S. Army Cold Regions Research and Engineering Laboratory, PO Box 35170, Fort Wainwright, AK 99703, USA.

A. Steffen, Air Quality Research Division, Environment Canada, 4905 Dufferin St., Toronto, Ontario M3H 5T4, Canada.